Experimental Evaluation of the Fatigue Performance and Self-Healing Behavior of Nanomodified Porous Asphalt Mixtures Containing RAP Materials under the Aging Condition and Freeze-Thaw Cycle

Mousavi Rad, Sina; Kamboozia, Neda; Anupam, Kumar; Saed, Seyed Ataollah

DOI
10.1061/(ASCE)MT.1943-5533.0004488

Publication date
2022

Document Version
Final published version

Published in
Journal of Materials in Civil Engineering

Citation (APA)
Mousavi Rad, S., Kamboozia, N., Anupam, K., & Saed, S. A. (2022). Experimental Evaluation of the Fatigue Performance and Self-Healing Behavior of Nanomodified Porous Asphalt Mixtures Containing RAP Materials under the Aging Condition and Freeze-Thaw Cycle. *Journal of Materials in Civil Engineering*, *34*(12), Article 04022323. https://doi.org/10.1061/(ASCE)MT.1943-5533.0004488

Experimental Evaluation of the Fatigue Performance and Self-Healing Behavior of Nanomodified Porous Asphalt Mixtures Containing RAP Materials under the Aging Condition and Freeze–Thaw Cycle

Sina Mousavi Rad[1]; Neda Kamboozia[2]; Kumar Anupam[3]; and Seyed Ataollah Saed[4]

Abstract: First, porous asphalt (PA) pavement possesses a lower strength and lifetime compared to typical dense-grade asphalt mixtures due to its large empty space structure. Second, PA pavements' fatigue life and durability are affected significantly by climate factors; the two most critical factors being aging conditions and moisture actions. Third, because of the environmental concerns connected with producing or repairing asphalt pavements using only virgin materials, studies have recommended reusing reclaimed asphalt pavement (RAP) materials. On the other hand, their use in road pavement is negative to the fatigue performance of asphalt pavements, especially PA. Therefore, modifying PA mixtures containing RAP to address the mentioned issues is necessary. Researchers have found that modifying asphalt mixes using nanotechnology is one of the more effective methods. The four-point bending beam fatigue test is one of the most dependable tests to assess the fatigue performance of asphalt mixtures, and evaluating the fatigue resistance of nano-modified PA mixes containing RAP under laboratory conditions by performing this test is essential. This study aims to investigate the fatigue behavior of different compounds of PA mixtures modified with nano zinc oxide (NZ) (0%, 2%, 4%, 6%, and 8%) containing various contents of RAP materials (0%, 25%, and 50%) under normal, long-term aging, and freeze–thaw (F–T) cycle conditions. Moreover, the self-healing capability of these PA samples was evaluated using this test by performing two 24-h recovery periods following the first and second loading. It can be inferred from the result that although adding RAP and inducting long-term aging and moisture-damaged conditions negatively influenced PA mixes' fatigue lives, incorporating NZ caused increases in these values by averages of 114%. Besides, results indicated that applied rest periods were observed to significantly impact PA specimens' self-healing capability, resulting in longer fatigue life for them. On average, conventional and NZ-modified PA mixes with/without RAP could recover up to 32 and 48% of their fatigue resistance in all conditions. **DOI: 10.1061/(ASCE)MT.1943-5533.0004488.**

Author keywords: Fatigue resistance; Porous asphalt (PA); Nano zinc oxide (NZ); Reclaimed asphalt pavement (RAP); Aging condition; Moisture damage; Self-healing; Four-point bending beam fatigue test.

Introduction

Porous asphalt (PA) mixtures have high air void contents (>20%), which are much more than the typical dense asphalt (DA) mixes (Mansour and Putman 2013; Zhang et al. 2020). In PA, an open-graded aggregate skeleton results in this large amount of air void (Al-Kaissi and Mashkoor 2016; Arshad et al. 2019; Poulikakos and Partl 2009). High permeability in the PA, rooted in a large empty space structure, allows rainfall to drain, decreases spray and splash, and increases driving comfort and safety (Anupam et al. 2014; Bolzan et al. 2001; Kandhal 2002; Slebi-Acevedo et al. 2020). Despite these advantages, the PA mixes have lower lifetimes (10 to 12 years) than dense-graded asphalt pavements, which can last up to 18 years (Voskuilen and Verhoef 2003). This could be attributed to the fact that the open structure of PA exposes a large bitumen surface area to oxygen and moisture. These factors speedup the aging process and damage the mixtures' bitumen aggregate bond, leading to different pavement distresses, such as fatigue cracking (Kandhal 2004; Poulikakos and Partl 2009; Wu et al. 2020). Besides, the presence of water in PA can have negative consequences if combined with other environmental factors, such as freeze–thaw (F–T) cycles (Breakah et al. 2009). Hence, improving the durability of PA by various modifier additives is critical in ensuring its long-term performance under environmental conditions (Zhang et al. 2021). In addition to all aforementioned, diminishing resources of aggregates and bitumen were the principal causes for incorporating recycled asphalt pavement (RAP) into conventional asphalt pavement such as PA (Goh and You 2012).

To cater to ever-growing traffic demand, highways are continuously built in various parts of the globe, resulting in increased use of aggregates and bitumen (Devulapalli et al. 2019; Ziari et al. 2019). On the other hand, the limitation of natural resources and the environmental concerns related to the disposal of waste pavement

[1]Master's Student, School of Civil Engineering, Iran Univ. of Science and Technology, Tehran 13114-16846, Iran. Email: sinamoosavirad@gmail.com

[2]Assistant Professor, School of Civil Engineering, Iran Univ. of Science and Technology, Tehran 13114-16846, Iran (corresponding author). ORCID: https://orcid.org/0000-0002-6625-7680. Email: nkamboozia@iust.ac.ir

[3]Assistant Professor, School of Civil Engineering, Delft Univ. of Technology, Postbus 5, 2600 AA Delft, Netherlands. Email: K.anupam@tudelft.nl

[4]Master's Student, School of Civil Engineering, Iran Univ. of Science and Technology, Tehran 13114-16846, Iran. ORCID: https://orcid.org/0000-0002-5051-171X. Email: ata.saed96@gmail.com

Note. This manuscript was submitted on December 14, 2021; approved on March 21, 2022; published online on September 20, 2022. Discussion period open until February 20, 2023; separate discussions must be submitted for individual papers. This paper is part of the ***Journal of Materials in Civil Engineering***, © ASCE, ISSN 0899-1561.

construction materials have promoted the use of RAP materials in the pavement construction process (Mansourkhaki et al. 2019). As a result of the decreased use of virgin bitumen and aggregates, reusing RAP materials to construct pavements has provided various environmental benefits (Gong et al. 2018; Moniri et al. 2021; Sun et al. 2019). However, the use of RAP materials comes with some performance drawbacks because a considerable proportion of aged binder in RAP material decreases the asphalt mixture's efficiency (Guo et al. 2020). For example, previous studies (Bharath et al. 2021; Mullapudi et al. 2020; Paluri et al. 2021) reported that asphalt mixtures' fatigue resistance containing RAP materials is rather low due to the aged and brittle bitumen. To address this issue, the addition of various additives such as rejuvenators can improve the limitation of RAP mixes (Guo et al. 2021). Besides, nanomaterials have been highly criticized for their capacity to enhance the productivity of asphalt mixtures containing RAP materials in the last few years (Kamboozia et al. 2021; Saed et al. 2022a).

Improving the bitumen by various additives is one method to enhance the properties of asphalt mixes, especially those containing RAP materials (Devulapalli et al. 2019). Nanotechnology has always been considered by researchers to modify the bitumen and asphalt mixes (Arshad et al. 2017, 2019). The addition of nanomaterials significantly improves asphalt mixture characteristics such as aging, fatigue, and moisture resistance (Guo and Zhang 2021; Li et al. 2017). Various nanoparticles such as nanosilica (NS), nano zinc oxide (NZ), nano titanium oxide, and others are being incorporated in asphalt construction as modifiers or additives to enhance asphalt pavements' mechanical behavior and long-term performances (Masri et al. 2021).

Kamboozia et al. (2021) assessed the effect of NS on the fatigue performance of stone matrix asphalt (SMA) mixtures containing RAP materials by performing the four-point beam fatigue test under the impact of mix conditioning. Results indicated that the addition of NS causes an increase in fatigue lives of RAP-containing SMA mixes. Zhang et al. (2018) evaluated the impacts of different NZ particle sizes on the rheological and mechanical performance of the bitumen and asphalt mixture. The authors indicated that the growth of NZ size in the bitumen deteriorates its creep stiffness and raises its ductility, softening point, antirutting factor, viscosity, and antiaging capability. Hamedi et al. (2016) investigated the moisture susceptibility of NZ-modified asphalt mixes. It can be inferred from the results that values of indirect tensile strength for the mixes modified with NZ were higher than the conventional mixtures. Moreover, several previous research studies (Badroodi et al. 2020; HasaniNasab et al. 2019; Wan et al. 2021) show that using various nano-modifiers increases the self-healing potential of asphalt mixtures.

The asphalt mix is a self-healing material (Castro and Sánchez 2006; Little and Bhasin 2007). The self-healing potential of asphaltic material has been investigated for the previous two decades with the goal of creating a sustainable asphalt pavement promoting green technologies (Xu et al. 2020). Various research studies have been conducted to evaluate the fatigue and self-healing behavior of samples under different test conditions such as with/without rest periods, under constant strain, and under constant stress conditions (Shafabakhsh et al. 2015; Shen and Sutharsan 2011). More than 90% of the distress in PA mixtures arises from a microcrack in the bitumen, indicating that the great majority of the damage in PA may be repaired using self-healing technologies (Xu et al. 2020). Van Dijk and Francken (Francken 1979; Van Dijk et al. 1972) found that introducing rest periods between continuous loading regimes reduces the fatigue of asphalt mixtures. Xu et al. (2020, 2021) evaluated different self-healing systems for PA mixes under the fatigue bending beam test. They observed that all self-recovery methods help porous asphalt to have a longer fatigue life. Badroodi et al. (2020) assessed the self-healing performance of NS-modified asphalt mix containing RAP materials. They found that using NS significantly improved the self-healing behavior of RAP-containing asphalt mixes.

Various research studies have been carried out in recent years to understand the effect of the nanomaterials on different types of asphalt mixture with or without RAP materials. Still, very limited studies have been conducted on nano-modified PA mixes containing RAP, especially under various laboratory conditions. Besides, not much attention has been paid to studying the effect of NZ on the long-term performance of asphalt mixtures. Considering the popularity that PA mixes have received in recent decades, the paper aims to explore the impact of the NZ modifier on the lifetime and self-recovery of PA mixtures with RAP under the aging condition and F–T cycle.

Objectives and Scope

As described, this study aims to investigate and analyze the different contents impacts of NZ on the fatigue resistance and self-healing capability of RAP-containing PA mixtures under various laboratory conditions such as (1) normal, (2) aging, and (3) F–T cycle. To achieve these goals, various PA beam specimens were prepared and evaluated through the four-point bending beam fatigue test. The aims of this research are summarized as follows:

- Investigating the effect of various contents of NZ modification and RAP materials on the fatigue performance of PA mixtures.
- Exploring and comparing the self-healing capability of conventional and NZ-modified PA mixtures with and without RAP materials.
- Evaluating the fatigue life values and self-recovery rates of NZ-modified PA mixes containing RAP under various conditions; normal, aging, and F–T cycle.
- Evaluating the parameters achieved from the four-point bending beam fatigue and self-healing tests using a statistical analysis approach.

Materials

Bitumen

A 60/70 penetration-grade bitumen obtained from Pasargad oil company was used as a base bitumen in this research, the features of which are presented in Table 1 which were determined according to ASTM D5M-20 (ASTM 2020b), ASTM D36M-14 (ASTM 2020d), ASTM D113-17 (ASTM 2017b), ASTM D4402M-15 (ASTM 2015), ASTM D70M-21 (ASTM 2021), ASTM D92-18 (ASTM 2018), and ASTM D1754M-20 (ASTM 2020a). The leading cause for choosing this type of bitumen was that it is ordinarily used in various regions (Saed et al. 2022b; Shafabakhsh et al. 2020).

Table 1. Features of the base bitumen

Properties	Unit	Standard	Result
Penetration	0.1 mm	ASTM D5M-20	68
Softening point	°C	ASTM D36M-14	46
Ductility	cm	ASTM D113-17	113
Rotational viscosity at 135°C	Pa.s	ASTM D4402M-15	0.33
Specific gravity	g/cm^3	ASTM D70M-21	1.018
Flash point	°C	ASTM D92-18	304
Mass loss	%	ASTM D1754M-20	0.11

Table 2. Properties of limestone aggregates

Properties	Unit	Standard	Requirements	Coarse aggregate (>4.75 mm)	Fine aggregate (<4.75 mm)
Los Angeles Abrasion	%	AASHTO T96-02	≤30	18	—
Flat and elongated (3 to 1)	%	ASTM D4791-19	≤20	8	—
Flat and elongated (5 to 1)	%	ASTM D4791-19	≤5	0.8	—
Absorption	%	AASHTO T85-14	≤2	1.2	—
Soundness, sodium sulfate	%	AASHTO T104-99	≤15	0.2	1.0
Liquid limit	%	AASHTO T89-13	≤25	—	18
Plasticity index	%	AASHTO T90-20	Non-plastic	—	Non-plastic
Sand equivalent	%	AASHTO T176-17	—	—	84

Table 3. The gradation of the limestone aggregates used in this study

Sieve size	19	12.5	9.5	4.75	2.36	0.75	Filler	Total
Passing requirement[a] (%)	100	85–100	55–75	12–25	5–10	2–4	0	—
Passing (%)	100	92.5	65	17.5	7.5	3	0	—
Retained (%)	0	7.5	27.5	47.5	10	—	3	100

[a]According to PWD Malaysia Standard Specification.

Aggregate

The aggregate materials used in this research were of a limestone type, and their properties are visualized in Table 2, which were determined according to AASHTO T 96-02 (AASHTO 2019), ASTM D4791-19 (ASTM 2019), AASHTO T 85-14 (AASHTO 2018), AASHTO T 104-99 (AASHTO 2020b), AASHTO T 89-13 (AASHTO 2017b), AASHTO T 90-20 (AASHTO 2020a), and AASHTO T 176-17 (AASHTO 2017c). According to PWD Malaysia Standard Specification for Road Works (Malaysia 2008), porous asphalt grading B was used for this research (Masri et al. 2016). Table 3 illustrates the gradation of aggregates used in this study.

RAP Materials

RAP materials used in this study were laboratory prepared through short-term and long-term aging processes. To define the RAP bitumen properties, the bitumen of RAP material was first dissolved in toluene, extracted according to ASTM D2172M-17 (ASTM 2017c), and then recovered using a rotary evaporator considering ASTM D5404M-12 (ASTM 2017a). The average bitumen content was determined at 5.2% by the weight of the total mass. Table 4 summarizes the RAP bitumen properties which were determined according to ASTM D5M-20 (ASTM 2020b), ASTM D36M-14 (ASTM 2020c), ASTM D113-17 (ASTM 2017b), and ASTM D4402M-15 (ASTM 2015). Moreover, the gradation of extracted RAP aggregates is presented in Fig. 1.

Table 4. Specification of the RAP bitumen

Properties	Unit	Standard	Result
Penetration	0.1 mm	ASTM D5M-20	68
Softening point	°C	ASTM D36M-14	46
Ductility	cm	ASTM D113-17	113
Rotational viscosity at 135°C	Pa.s	ASTM D4402M-15	0.33

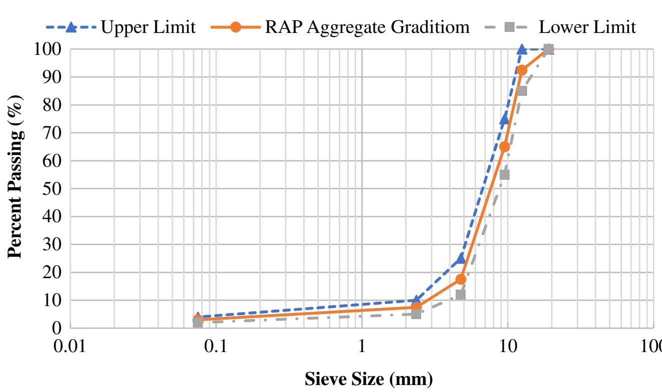

Fig. 1. The RAP aggregates' gradation.

Nano Zinc Oxide

The zinc oxide (ZnO) particle has several unique features and is readily available. As a result, numerous studies on the use of ZnO nanoparticles in bitumen and asphalt mixture have been conducted. The solvent technique and mechanical agitation make ZnO-modified asphalt with excellent characteristics (Guo and Zhang 2021; Zhang et al. 2015). The chemical compositions and physical features of NZ used in this research are summarized in Table 5. In this study, various percentages of NZ (0%, 2%, 4%, 6%, and 8% by the total weight of bitumen) were used. Fig. 2 visualizes the scanning electron microscope (SEM) image of NZ.

Cellulose Fiber

To prevent drain-down, it is necessary to use a specific additive in open-gradation asphalt mixtures as porous asphalt, which owns a higher bitumen amount of bitumen with a low amount of filler (Kamboozia et al. 2021). In this research, 0.3% TOPCEL cellulose fiber by the weight of the total mix according to the AASHTO M 325-08 (AASHTO 2017d) was used, which was directly added to the asphalt mixtures. Table 6 summarizes the features of TOPCEL cellulose fiber used in this study.

Methodology

The research framework of this study is presented in Fig. 3. The first step was to prepare artificial RAP, NZ, and other materials.

Table 5. Physical properties of NZ

Properties	Unit	Result
Molecular formula	—	ZnO
Purity	%	98
Bulk density	g/cm^3	5.6
Color	—	White
Size of particles	Nm	40
Loss on ignition	%	1
Melting point	°C	1,975
Molecular weight	g/mol	81.38
Morphology	—	Hexagonal
Flash point	°C	1,430
Boiling point	°C	2,360

J. Mater. Civ. Eng., 2022, 34(12): 04022323

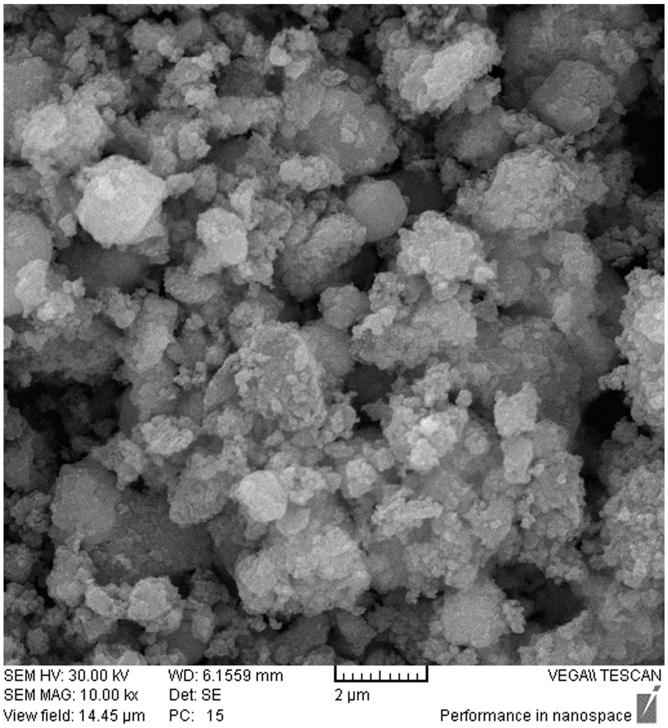

Fig. 2. The SEM image of NZ (nano-ZnO) used in this study 10,000 × magnification.

Table 6. The properties of TOPCEL

Standard analysis	Unit	Value
Fiber content	%	95 ± 3
Natural wax	%	1.5–2.5
Average fiber length	mm	15
Average fiber thickness	mm	4.5
Bulk density	g/L	420–480
Moisture content	%	≤6.0
Residue on ignition	%	10–20

The following step was started by mixing various percentages of NZ (0%, 2%, 4%, 6%, and 8%) with the base bitumen by a high-shear mixer. Then, the various samples of PA beam mixtures containing 0%, 25%, and 50% RAP materials with unmodified and nano-modified bitumen were fabricated in the following. For manufacturing PA beam specimens, design bitumen contents (DBC) in porous asphalt mixtures with different NZ percentages were defined (Kamboozia et al. 2022).

In the next step, all of the PA beam samples were divided into three groups. The first group was named "Normal." The second group was called "Long-Term Aged," in which the specimens were put in the heater for 5 days at 85°C to induct the aging condition (Ziari et al. 2020b). One-third of specimens were subjected to moisture damage which was grouped as the F–T cycle. F–T conditioned samples were saturated by a vacuum and then were put into a chamber for 16 h and frozen in the air with a temperature of −18°C. Afterward, the samples were thawed in a hot water bath with a temperature of 60°C for 16 h, and finally, samples were kept in water at 25°C for 2 h (Xu et al. 2015, 2016). As can be shown in Fig. 4, long-term aging has a significant impact on the appearance of PA mixtures. The processes of the F–T cycle are visualized in Fig. 5. In the last step, all the samples were tested by the four-point bending beam fatigue test for evaluating the fatigue life of PA mixtures containing RAP materials with modified and unmodified bitumens.

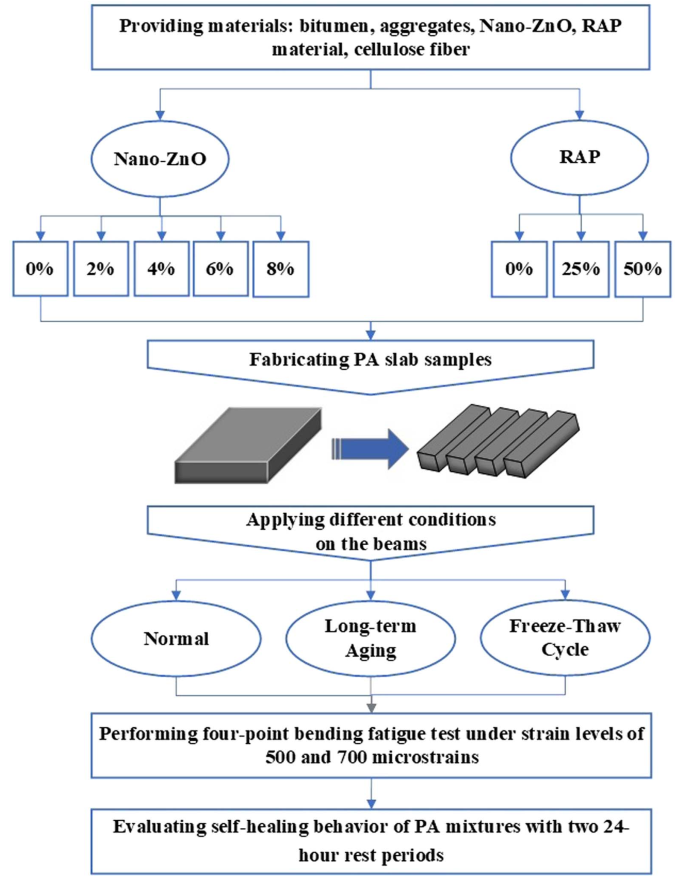

Fig. 3. Summary of experimental framework.

Fig. 4. PA beam samples: (a) unaged; and (b) long-term aged.

In this stage, all specimens were tested by the four-point bending test, but half of them were tested with two 24-h rest periods that were performed after the first and second loading to evaluate the self-healing behavior of PA mixtures (Badroodi et al. 2020). Different codes were assigned to various compounds of PA mixtures, as shown in Table 7, in order to make reporting easier.

Modified Bitumen Preparing

For mixing nanoparticles into the base bitumen, a high-shear mixer at a rate of above 4,000 rpm was used in this study. The wet method was used to combine the nanoparticles into bitumen in this research, so the NZ was first dispersed into the solver. The choice of solver depended upon the following: (1) the solver should be able to solve bitumen at moderate temperatures without affecting the bitumen features; and (2) to uniformly incorporate NZ into bitumen, the solver should have a low viscosity at room temperature. In

(a) (b) (c)

Fig. 5. The F–T cycle process: (a) covering the beam samples after saturating by vacuum; (b) putting in a chamber with 18°C temperature; and (c) putting in a hot water bath with 60°C temperature.

this study, kerosene was taken as a solver (Kordi and Shafabakhsh 2017). At the first stage, various contents of NZ (2%, 4%, 6%, and 8% by the weight of bitumen) were dissolved in the kerosene. Then, those mixtures were added slowly to the base bitumen at the temperature of 150°C while the mixer was rotating at the rate of 4,000 rpm, kept for 15 min. Following this, the mixture was sheared at 6,000 rpm for 30 min (Saed et al. 2022a). To evaporate the remaining solver, the homogenous mix of bitumen and nanoparticles was left at room temperature (Sadeghnejad and Shafabakhsh 2017). In this research, the NZ was first added to the base bitumen. After that, the NZ modified bitumen was added to the mix of aggregates and RAP materials.

Fig. 6 illustrates the SEM images of conventional and NZ-modified bitumen in the mentioned order. The SEM test is one of the best methods to demonstrate the efficacy of nano-modified materials mixing operations. An SEM can capture pictures at the nanoscale to show combining quality (Behbahani et al. 2015). It can be seen from Fig. 6(c) that the NZ modifier indicates a significant inclination for aggregation with constructing a random network of interacting particles. To fully utilize the potential of NZ as a bitumen modifier, it is essential to scatter these nanoparticles as much as possible in the bitumen. As demonstrated in Fig. 6(d), the blending successfully mixed NZ in bitumen and created an NZ–bitumen matrix.

Asphalt Mix Design and Specimen Preparation

The DBC of PA mixtures containing 0%, 25%, and 50% RAP materials was assessed based on the Marshall method as 5.32%, 3.73%, and 2.56%, in the mentioned order. The bitumen drain-down, Cantabro loss, and air void content test were performed to define the optimum bitumen content in porous asphalt samples (Kamboozia et al. 2021; Ma et al. 2018). To determine DBC, the cylindrical samples were fabricated by Superpave Gyratory Compactor (SGC) with a diameter of 100 mm, and an approximate height of 70 mm. Table 8 presents the results of DBC and PA performance tests which were determined according to ASTM D3203 (ASTM 2011), AASHTO T 305 (AASHTO 2014), and ASTM C131 (ASTM 2020c).

For fabricating PA beam samples, RAP materials and virgin aggregates were held at mixing temperature for 2 and 16 h, in the same order (Kamboozia et al. 2021; Saed et al. 2022a). Afterward, RAP materials, virgin aggregates, and cellulose fibers were mixed together, and then optimum contents bitumen was added (Daryaee et al. 2020; Ziari et al. 2020a). Eventually, the uncompacted PA mixes were cured for 2 h at the compaction temperature before compacting to the target air void with a Roller Wheel Compactor (Yousefi et al. 2021). Finally, after fabricating PA slab samples, each was cut into four PA beams with dimensions of $50 \times 63 \times 380$ mm by a circular and sharp saw, and water was utilized as a cooling fluid to prevent the saw from failing to the warming effect (Shadman and Ziari 2017).

The Test Methods

Four-Point Bending Beam Fatigue Test

To evaluate the fatigue performance of asphalt mixtures, a Beam Fatigue Test (BFT) is considered one of the most trustworthy tests (Daryaee et al. 2020). The main goal of this test (carried out by using standard beam-shaped samples) is to develop a model for the fatigue life prediction of asphalt mixtures at 50% initial flexural stiffness. The number of load cycles to failure (Nf50) in BFT is calculated as the number of cycles needed to achieve a 50% reduction in initial stiffness. This machine can repeatedly apply bending loads to asphalt samples while assessing the applied load and deformation. The rectangular asphalt beam was subjected to a continuous bending flexural loading at a particular strain level for the fatigue test. This test was conducted at different temperatures, strain levels, and loading frequencies according to AASHTO T 321-17 (AASHTO 2017a). In this study, BFT was performed at 20°C, strain levels of 500 and 700 microstrains, and a loading frequency of 10 Hz according to some studies (Daryaee et al. 2020; Shadman and Ziari 2017). Before starting the test, specimens were held in the chamber for four hours at 20°C. The test setup in this study is illustrated in Fig. 7.

Table 7. The codes of different compounds of mixtures

Mixture code	Mix design of the mixture
0N0R-N	0%NZ + 0%RAP materials + normal condition
0N25R-N	0%NZ + 25%RAP materials + normal condition
0N50R-N	0%NZ + 50%RAP materials + normal condition
0N0R-A	0%NZ + 0%RAP materials + long-term aging
0N25R-A	0%NZ + 25%RAP materials + long-term aging
0N50R-A	0%NZ + 50%RAP materials + long-term aging
0N0R-F	0%NZ + 0%RAP materials + F-T cycle
0N25R-F	0%NZ + 25%RAP materials + F-T cycle
0N50R-F	0%NZ + 50%RAP materials + F-T cycle
2N0R-N	2%NZ + 0%RAP materials + normal condition
2N25R-N	2%NZ + 25%RAP materials + normal condition
2N50R-N	2%NZ + 50%RAP materials + normal condition
2N0R-A	2%NZ + 0%RAP materials + long-term
2N25R-A	2%NZ + 25%RAP materials + long-term
2N50R-A	2%NZ + 50%RAP materials + long-term
2N0R-F	2%NZ + 0%RAP materials + F-T cycle
2N25R-F	2%NZ + 25%RAP materials + F-T cycle
2N50R-F	2%NZ + 50%RAP materials + F-T cycle
4N0R-N	4%NZ + 0%RAP materials + normal condition
4N25R-N	4%NZ + 25%RAP materials + normal condition
4N50R-N	4%NZ + 50%RAP materials + normal condition
4N0R-A	4%NZ + 0%RAP materials + long-term
4N25R-A	4%NZ + 25%RAP materials + long-term
4N50R-A	4%NZ + 50%RAP materials + long-term
4N0R-F	4%NZ + 0%RAP materials + F-T cycle
4N25R-F	4%NZ + 25%RAP materials + F-T cycle
4N50R-F	4%NZ + 50%RAP materials + F-T cycle
6N0R-N	6%NZ + 0%RAP materials + normal condition
6N25R-N	6%NZ + 25%RAP materials + normal condition
6N50R-N	6%NZ + 50%RAP materials + normal condition
6N0R-A	6%NZ + 0%RAP materials + long-term
6N25R-A	6%NZ + 25%RAP materials + long-term
6N50R-A	6%NZ + 50%RAP materials + long-term
6N0R-F	6%NZ + 0%RAP materials + F-T cycle
6N25R-F	6%NZ + 25%RAP materials + F-T cycle
6N50R-F	6%NZ + 50%RAP materials + F-T cycle
8N0R-N	8%NZ + 0%RAP materials + normal condition
8N25R-N	8%NZ + 25%RAP materials + normal condition
8N50R-N	8%NZ + 50%RAP materials + normal condition
8N0R-A	8%NZ + 0%RAP materials + long-term
8N25R-A	8%NZ + 25%RAP materials + long-term
8N50R-A	8%NZ + 50%RAP materials + long-term
8N0R-F	8%NZ + 0%RAP materials + F-T cycle
8N25R-F	8%NZ + 25%RAP materials + F-T cycle
8N50R-F	8%NZ + 50%RAP materials + F-T cycle

Self-Healing Capability Measurement

The self-healing capabilities of asphalt mixes were evaluated by their flexural stiffness. The flexural stiffness of the asphalt pavement was reduced by increasing their lifespan. However, the flexural stiffness could be considerably recovered to its previous rate if a sufficient period is given for self-healing (Badroodi et al. 2020; Kim et al. 2003). Thus, the specimens in this research were given two 24-h rest times after the first and second loading. This process consists of three stages that result in partial or complete healing of the asphalt bitumen's natural mechanical characteristics over the fragmented surface (crack). These three steps happen in two phases: (1) the viscoelastic self-healing phase, which includes linking the aggregate surface to the bitumen, and (2) the viscose self-healing phase, which is time-dependent and correlates to bitumen material cohesion. Two close fractured surfaces in nanoscale materials can potentially adhere if pressure and temperature are applied at the nanoscale size. In that case, the chemical bonds will be formed at the joint level, and the crack recovery will occur. For measuring the self-healing values of different compounds of PA mixes in this research, the ratio of flexural stiffness in stage 3 (FS_3) to flexural stiffness in stage 1 (FS_1) was calculated and compared with each other after BFT with two 24-h rest periods (Badroodi et al. 2020).

Results and Discussion

Beam Fatigue Test Results

Figs. 8 and 9 illustrate the four-point bending beam fatigue test results on the conventional and NZ modified PA samples containing RAP materials at strain levels of 500 and 700 microstrains under the normal, F–T cycle, and long-term aging conditions at a temperature of 20°C. As can be expected, the results show that the fatigue life was inversely proportional to the strain levels and RAP contents. As the strain level increased from 500 to 700 microstrains or RAP content rose from 0 to 50%, respectively, the resulting fatigue life became shorter. Meanwhile, the fatigue life value was directly proportional to the NZ content in all conditions and both strain levels. Thus, along with the addition of NZ, the fatigue life value increased. This means that the fatigue performance of PA mixtures was considerably enhanced due to adding the NZ additive. Besides, it can be observed from the results that the F–T cycle and long-term aging conditions negatively affected the fatigue resistance of PA mixtures. This evidence shows that the fatigue lives of long-term aged and water-damaged PA samples were lower than that of normal samples.

According to Figs. 8 and 9, when the strain level climbed from 500 to 700 microstrains, the fatigue life values of modified/unmodified PA mixtures with/without RAP materials decreased by an average of 75.9%, 62.5%, and 69% in the normal, F–T cycle, and long-term aging conditions, respectively.

Regarding the effect of RAP materials on the fatigue performance of PA mixtures, the fatigue life values of different compounds were reduced when RAP materials were added to the reference mixture. Also, as seen in these graphs, samples with a higher percentage of RAP have a shorter fatigue life compared to those with less RAP content. This is due to the fact that RAP materials contain aged bitumen, which allows the whole mixture to become much stiffer and harder than mixtures containing virgin bitumen and aggregates, resulting in RAP-contained mixtures having shorter fatigue life. The fatigue life values of 0N0R-N, 0N0R-F, and 0N0R-A at both strain levels were diminished by averages of 30.61%, 33.4%, and 27.62% by adding 25% RAP and 61.47%, 65.42%, and 56.88% by addition of 50% RAP, respectively.

Results show that adding NZ to PA mixtures in all conditions and RAP contents increased the fatigue resistance. The addition of NZ caused the fatigue lives of the samples in the conditions of normal, water action, and aging to be higher by averages of 283.33%, 277.14%, and 265.11% at a strain level of 500 microstrains compared to unmodified PA mixtures, respectively. This is while these values at the strain level of 700 microstrains were 276.47%, 248.57%, and 190.77%, in the mentioned order. This can be explained by the fact that the addition of NZ to the bitumen enhances the interaction between the nanoparticles and the functional groups of the bitumen, resulting in forming a network within the structure of the bitumen and delaying the appearance of microcracks in asphalt mixtures (Li et al. 2015, 2017). Another explanation could be that NZ strengthens bitumen particles due to its high surface–volume ratio. Thus, the aforementioned factors can increase bitumen viscosity and adhesion, improve bitumen's functional behavior, and reduce its fatigue sensitivity.

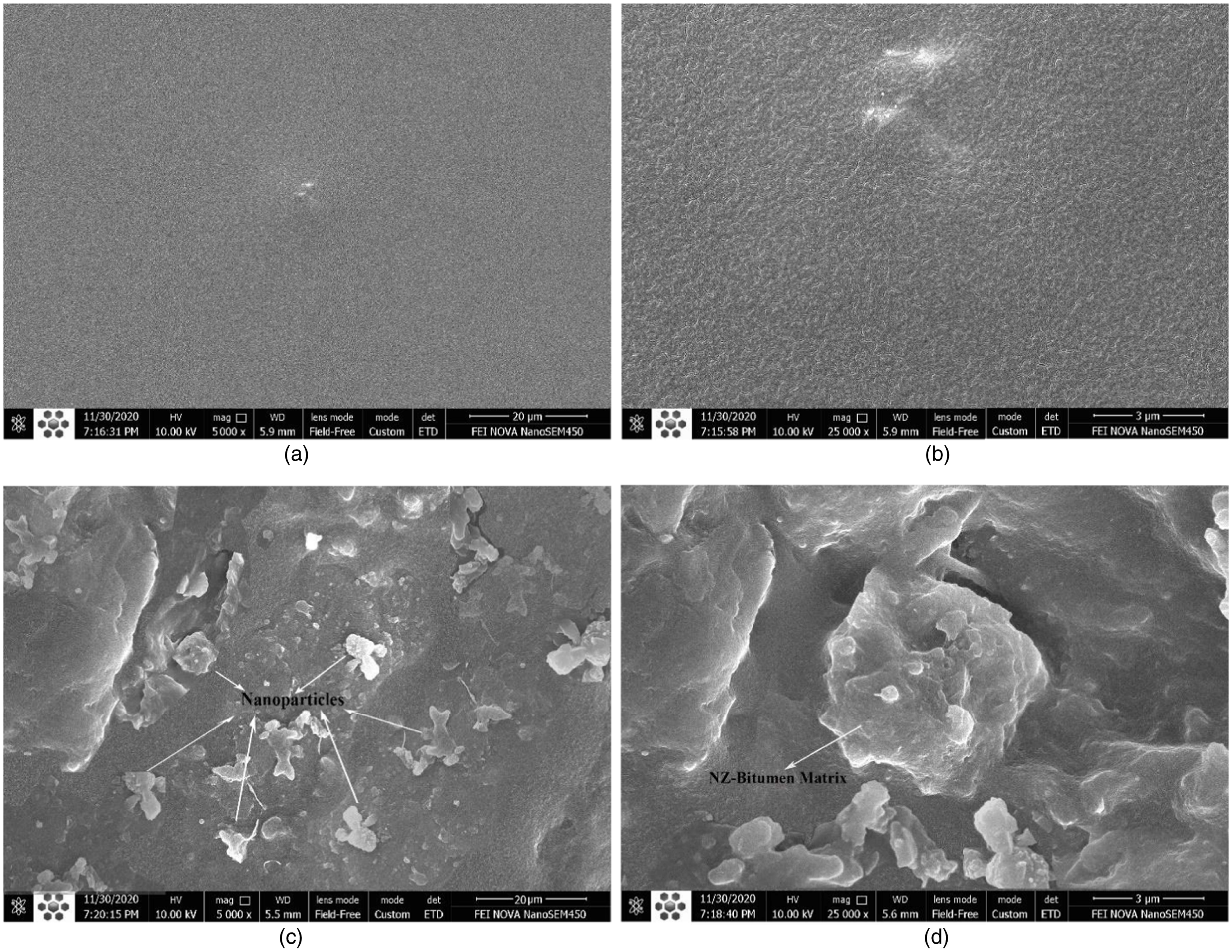

Fig. 6. SEM images of conventional (a and b) and nano-modified (c and d) bitumens: (a and c) 5,000 × magnification; and (b and d) 25,000 × magnification.

Table 8. Results of porous asphalt performance tests

RAP content	DBC (%)	Tests/allowable values/standard: Air void ≥ 18% ASTM D3203 (ASTM 2011)	Drain-down ≤ 0.3% AASHTO T 305 (AASHTO 2014)	Cantabro ≤ 25% ASTM C131 (ASTM 2020c)
PA–0% R	5.32	19	0.194	9.83
PA–25% R	3.73	18.6	0.151	13.2
PA–50% R	2.56	18.9	0.117	17.56

It can also be observed from Figs. 8 and 9 that PA specimens containing more than 6% NZ had shorter fatigue lives than the specimens containing 6% NZ or less. This reduction is justified because as the content of NZ increases from 6% to 8%, the distance between the bitumen particles gradually increases. As a result, the strength of bitumen particles decreases, because the increased distance between the bitumen molecules reduces gravitational force between them and consequently causes to diminish the adhesion and cohesion of the bitumen. Therefore, the particles' cohesion and adhesion are broken with the least amount of force, and the bitumen loses its adhesion capacity.

As shown in Figs. 8 and 9, specimens comprising RAP materials and modified with NZ have better fatigue resistance than unmodified ones. As can be seen on these figures, regardless of the applied strain level, 2N25R-N, 2N25R-F, and 2N25R-A have longer fatigue lives than their reference mixtures, 0N25R-N, 0N25R-F, and 0N25R-A, respectively. At both strain levels, the NZ modified PA mixtures containing 25% and 50% RAP have an average 200.1% and 196.75% longer fatigue life than the unmodified mixtures containing 25 and 50% RAP materials.

From Figs. 8 and 9, it can be observed that the long-term aging process and the F–T cycle had adverse effects on the fatigue performance of all conventional and modified PA mixtures with/without RAP materials. This indicates that long-term aged and moisture-inducted PA specimens had shorter fatigue lives compared to unconditioned samples. This could be associated with the fact that the

Fig. 7. The beam fatigue test setup.

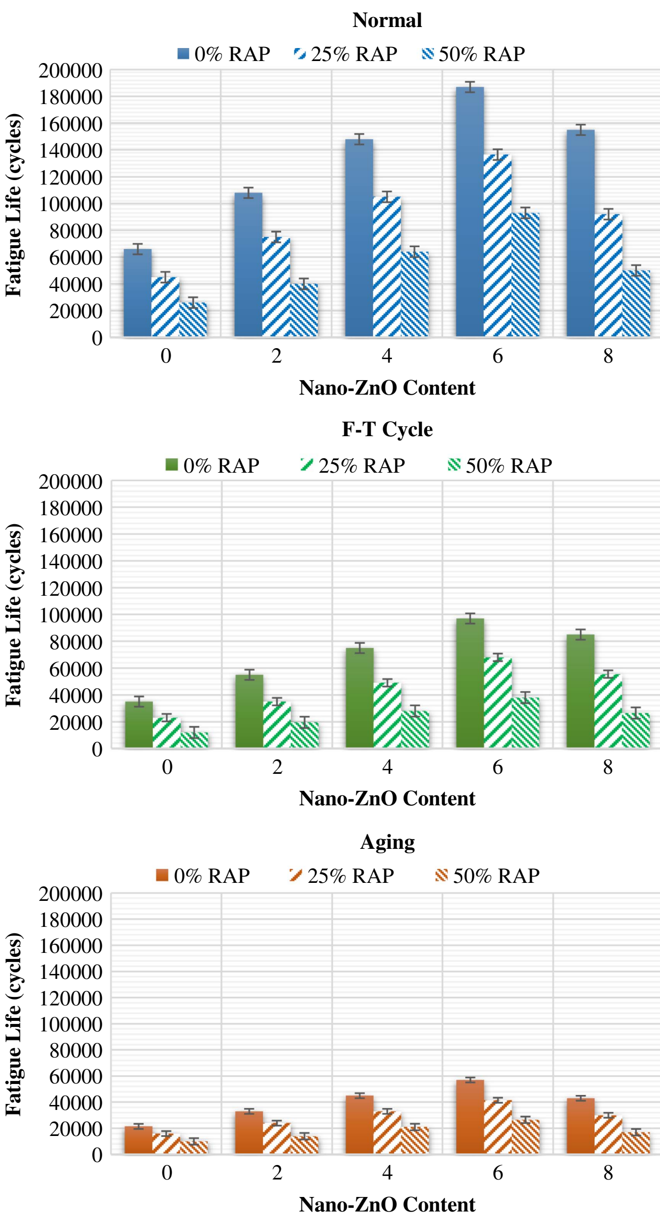

Fig. 8. The fatigue lives of PA mixes at the strain level of 500 microstrains.

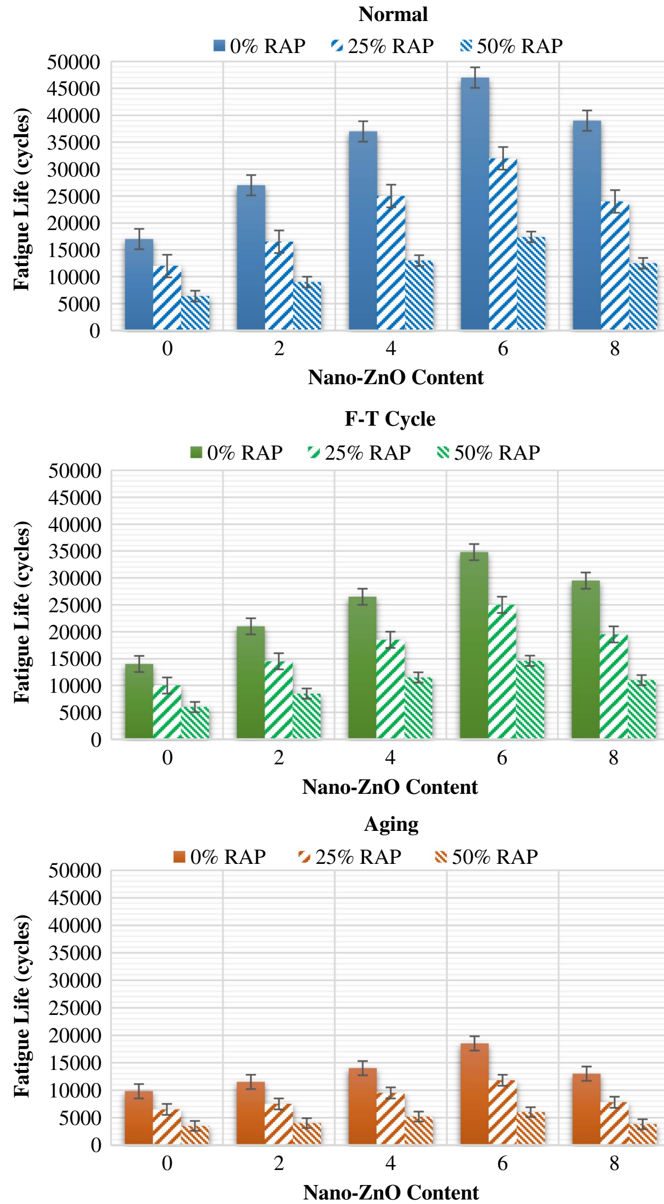

Fig. 9. The fatigue lives of PA mixes at the strain level of 700 microstrains.

aging process made the bitumen stiffer. Thus, the aged samples were less resistant to fatigue. Also, The F–T cycle weakened bonds between bitumen and aggregate particles, which made samples susceptible to failure. It should be noted that the F–T cycle and long-term aging decreased the fatigue life of conventional PA mixtures on averages of 30.285 and 53.88 regardless of strain levels, respectively. As can be evident from these results, the fatigue performance of the asphalt mixture is relatively much affected by the phenomenon of aging. However, it can be inferred from the figures that the amount of increase in the effect of the aging on the fatigue behavior of PA mixtures containing RAP (8.22%) was less than the amount of growth in the impact of the F–T cycle on RAP containing mixtures (15.26%) compared to that of without RAP. This can be explained by the fact that RAP materials have been subjected to significant aging throughout their lives, and further aging in the laboratory has a smaller impact on their fatigue life than mixes without RAP. Moisture is considered a more damaging phenomenon on the fatigue performance of mixtures containing RAP materials.

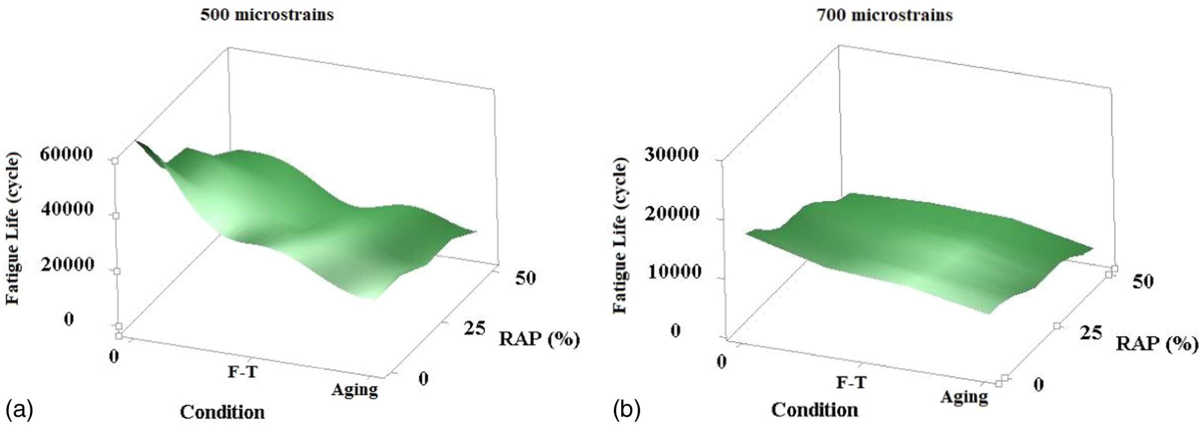

Fig. 10. The 3D plot of fatigue life versus various RAP materials contents and conditions of PA mixes at strain levels of (a) 500; and (b) 700 microstrains.

Fig. 10 presents the three-dimensional (3D) plot of fatigue lives of conventional and NZ modified PA mixtures versus various RAP materials contents and conditions at strain levels of 500 and 700 microstrains. It can be inferred from Fig. 10(a) that the effect of conditions on diminishing the fatigue life of PA mixtures was significantly higher than the RAP materials' effect at the strain level of 500 microstrains. In contrast, as shown in Fig. 10(b), the fatigue performance of PA samples was affected more by RAP contents rather than the conditions at 700 microstrains. It can be inferred from the above discussion that the presence of RAP materials and their contents in PA mixtures is more critical at higher strain levels.

Self-Healing Results

Figs. 11 and 12 illustrate the flexural stiffness variations of unmodified and NZ modified PA mixtures containing different RAP contents in normal condition under strain levels of 500 and 700 microstrains. The flexural stiffness of the PA specimens was reduced by increasing their lifespan. This is seen in all samples with/without RAP materials and nanoparticles content, irrespective of test conditions. From Figs. 11 and 12, the mechanical parameters such as stiffness and resistance were recovered caused by crack widening during the rest time. Rest times were found to have a considerable impact on the self-healing capability of the porous asphalt pavement, which enhanced fatigue resistance and increased fatigue life. Fig. 11 indicates that the base bitumen has a self-healing property; if a sufficient resting time is taken into account, this intrinsic feature of crack healing can extend the PA pavement's service life. That is, two close broken edges in nanoscale solids have the propensity for adhesion. Chemical bonds will establish at the joint layer, and crack healing will occur if two surfaces in the nanometer dimensions come into contact with heat and pressure. Besides, it can be observed from Fig. 12 that the addition of NZ efficiently inhibits crack development and consequently improves the self-recovery capability. That is because the NZ modifier has a high propensity for moving toward damaged areas of the PA samples due to its high specific surface, hastening the self-healing of cracks. In other words, the cracks will be closed, resulting in a longer fatigue lifespan for the pavement. It can also be concluded that if the nano-modified specimens are given sufficient time to rest, they will restore their mechanical characteristics completely.

As shown in Figs. 11 and 12, the PA samples' flexural stiffness increases as the amount of RAP was increased. This could be

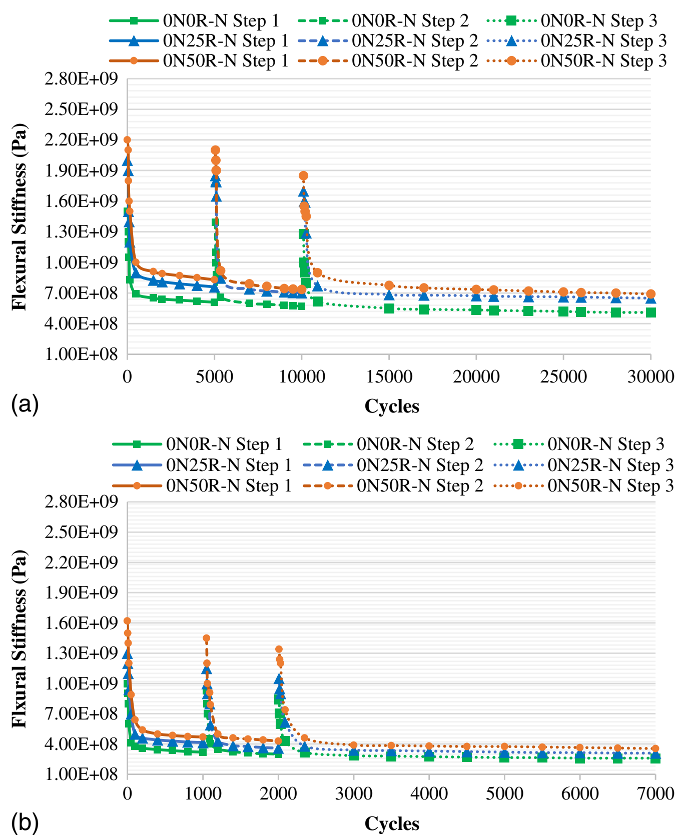

Fig. 11. Flexural stiffness variations in unmodified normal PA samples containing various RAP contents under strain levels of (a) 500; and (b) 700 microstrains.

associated with the fact that RAP materials had higher stiffness due to aging. Furthermore, self-healing is more visible at the lower strain level (500 microstrains) due to a lower accumulated level of destruction. Also, as the strain increases, the speed of self-healing decreases. It can be explained by the fact that the rate of self-healing is proportional to the total amount of damage. It can be inferred that the higher strain level (700 microstrains) speeds up the process of destruction and limits the ability of asphalt particles to heal in a short period. Under strain levels of 500 and 700

J. Mater. Civ. Eng., 2022, 34(12): 04022323

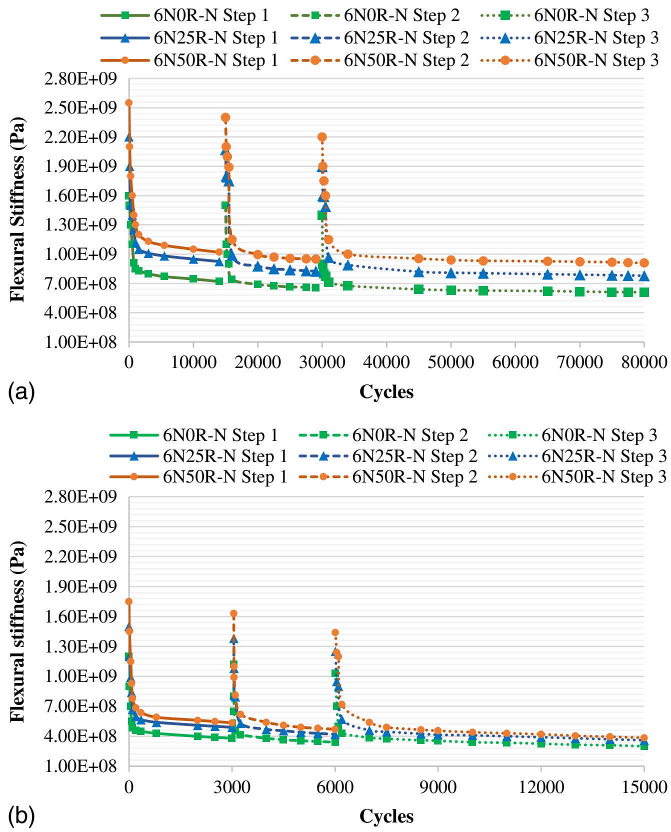

Fig. 12. Flexural stiffness variations in 6% nano-modified normal PA samples containing various RAP contents under strain levels of (a) 500; and (b) 700 microstrains.

microstrains, the self-healing behaviors of all PA mixes were significantly different in various conditions.

Fig. 13 presents the self-healing rate in all PA specimens containing different contents of nanoparticles and RAP materials under various conditions. The recovery propensity is indicated as a reduction in stiffness as compared to the initial stiffness. It is clear that the healed specimens improved their flexural stiffness significantly.

It can be inferred from Fig. 13 that because of the time allocated for strain healing and the micro-cracks, the self-healing values of all PA mixes were considerably boosted by averages of 15.4% at the lower strain level (500 microstrains). It could be associated with the fact that the process of self-healing rate is a function of the accumulated amount of destruction; as strain rises, the self-healing ratio drops. Thus it can be concluded that a high level of strain will speed up the process of damage and restrict the ability of asphalt compounds to reclaim in a shorter time (Badroodi et al. 2020).

Fig. 13 shows that the adverse test conditions, the F–T cycle, and long-term aging negatively influence the self-healing capability of PA mixes. This could also be explained by the fact that the moisture and aging process leads to reductions in the rates of PA's self-healing capabilities. On average, the reductions are 19.55% and 46.6%, respectively, due to moisture and aging at the strain level of 500 microstrains compared to unconditioned PA specimens. The decrement is even higher at a higher strain value of 700 microstrains at 21.5% and 47.56%, respectively. It can be concluded that the effect of aging on diminishing self-healing rates was significantly higher than the impact of moisture damage.

From Fig. 13, it can be seen the self-healing capability of PA mixes containing RAP materials had far lower rates compared to those without RAP. An addition of 25% and 50% RAP to the PA mixtures on average decreased the self-healing values in all conditions by 18.4% and 36.75% at the strain level of 500 microstrains. At a higher strain value of 700 microstrains, the decrements are about 24.9% and 42.77%, in the same order. It should be noted that the effect of RAP in decreasing the self-healing rate in moisture inducted PA samples, which was 37.75%, was higher than in long-term aged specimens, being 31.5%. This is because, as aforementioned, RAP materials have been exposed to substantial aging throughout their lifetimes, and subsequent aging in the laboratory has a lesser influence on their fatigue behavior than mixtures that do not contain RAP.

It is evident from Fig. 13 that adding NZ to the PA mixtures with/without RAP materials significantly increases the rates of self-healing. Fig. 13 also indicates that PA mixtures showed different self-healing behaviors with various NZ and RAP content. For example, 6N0R-N and 6N25R-N had self-healing values 161.1% and 147.25% higher than that of unmodified samples, respectively. In contrast, the self-healing rate of the 4N50R-N mix was an average 142.64% higher than that of the 0N50R-N mix regardless of strain level. Besides, in the condition of the F–T cycle, the addition of 8% NZ increased the self-healing rates of moisture-induced PA samples with 0 and 25% RAP to be 149.5% and 146.35% higher as compared to the unmodified mixtures. However, the self-healing rate of 0N50R-F was on an average 143.5% higher than unmodified 50% RAP-contained specimens. Furthermore, the highest self-healing values in the long-term aging condition were seen in 4N0R-A and 4N25R-A, 138.2% and 134.15% higher than the self-healing rates in 0N0R-A and 0N25R-A, in the mentioned order on average at both strain levels. Conversely, the self-healing rate of 50% RAP containing aged PA specimens showed its highest value when modified with 2% NZ.

Statistical Analysis

In this research, an ANOVA tool was used to determine how each variable influences the fatigue life and self-healing performance results. Variables were NZ content, RAP materials, conditions, and strain levels. In this study, a confidence level of 95% was considered sufficient to satisfy the ANOVA method. The results of this analysis are summarized in Table 9.

Two statistically important parameters, *P*-value and *F*-value, were considered as acceptance/rejection criteria. *P*-value determines if a parameter has a significant influence on the outcome of each test. It is noted that if the *P*-value for a parameter is less than 0.05 for the confidence level of 95%, it should be accepted. The *F*-value lists the variables according to their degree of importance. The higher the *F*-value, the more influential the parameter is.

Table 9 shows that the *P*-value for each parameter is less than 0.05, which shows that no variable is determined to have an insignificant impact on the outcomes. As shown in Table 9, the applied strain level had the most significant effect on fatigue damage resistance, followed by the condition. The self-healing behavior of PA mixes was influenced significantly by the condition, followed by the RAP content. Besides, it should be mentioned that, as can be expected before in 3D plots of beam fatigue test, the condition variable was discovered to be the most effective parameter. It is noted that the RAP content ranked first regarding its effectiveness on the PA mix's fatigue life value.

Conclusions

The study presented the test results and analysis of the effect of NZ modifier and RAP materials on PA's fatigue behavior and

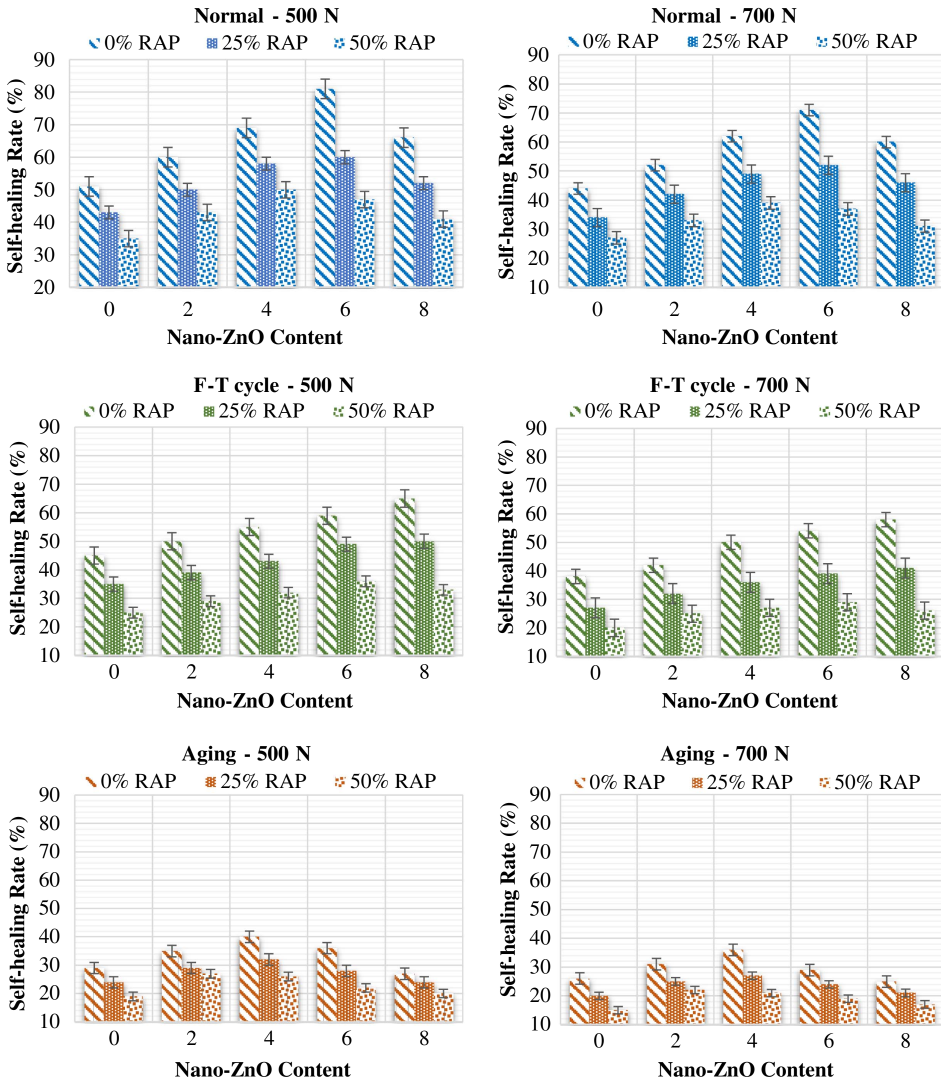

Fig. 13. Comparison of self-healing value in various compounds of PA specimens inducted different conditions under the diverse constant strain levels.

Table 9. The ANOVA results for the impact of RAP content, NZ content, conditions, and strain level on the performance of PA mixtures

Source	Adjusted sum of squares	Adjusted mean square	F-value	P-value	Acceptance
Fatigue life (total)					
NZ content	11,866,277,111	2,966,569,278	7.94	0.000	Accept
RAP content	15,125,750,889	7,562,875,444	20.22	0.000	Accept
Condition	23,151,773,556	11,575,886,778	30.98	0.000	Accept
Strain level	35,696,641,778	35,696,641,778	95.54	0.000	Accept
Fatigue life (500 microstrains)					
NZ content	15,198,077,778	3,799,519,444	13.59	0.000	Accept
RAP content	17,537,733,333	8,768,866,667	31.36	0.000	Accept
Condition	32,552,133,333	16,276,066,667	58.21	0.000	Accept
Fatigue life (700 microstrains)					
NZ content	947,963,111	236,990,778	14.18	0.000	Accept
RAP content	1,722,208,444	861,104,222	51.53	0.000	Accept
Condition	1,409,067,111	704,533,556	42.16	0.000	Accept
Self-healing					
NZ content	1,611.2	402.81	17.74	0.000	Accept
RAP content	5,490.2	2,745.10	120.87	0.000	Accept
Condition	8,454.1	4,227.03	186.12	0.000	Accept
Strain level	921.6	921.6	40.58	0.000	Accept

self-healing capability. The influence of the F–T cycle and aging condition on fatigue behavior and self-healing capabilities were also examined. The fatigue resistance of PA beam samples was evaluated using the four-point bending beam fatigue test, and self-healing performance was assessed using this test by performing two 24-h rest periods after the first and second loading. Finally, the most significant variables in the acquired results were determined using the ANOVA statistical approach. In general, the following conclusions can be drawn:

- Self-healing and fatigue life was found to be influenced by the applied loading condition. It was observed that self-healing tendency and expected fatigue life was maximum when at the lower strain level (500 microstrains).
- Rest times were found to impact self-healing potential substantially, consequently boosting fatigue resistance and extending the fatigue life of the porous asphalt. Therefore, it might be argued that implementing the rest period will increase the self-healing mechanism and, in consequence, enhance fatigue life.
- Considering the effect of the NZ modifier on the fatigue resistance and self-healing performance of porous asphalt mixtures, it can be concluded that the addition of NZ led to an increase in the fatigue life and self-recovery capability of PA beam samples significantly. Furthermore, it should be noted that all modified PA specimens with/ without RAP materials had higher fatigue life and self-healing values than the unmodified samples. It was also observed that 6% NZ is optimal for PA mixtures in long-term performance.
- It was also observed that using RAP causes fatigue life and self-recovery to significantly reduce on average 46% and 30%, respectively.
- It was observed that the F–T cycle and long-term aging conditions significantly affect the fatigue resistance and self-recovery capability of PA samples in terms of negative. Besides, results further showed that the impact of the aging process on diminishing the mentioned parameters was higher than the moisture action effect.
- The ANOVA tool showed that among all variables, the applied strain level and condition were the most influential factors in fatigue and self-healing results, respectively.

In general, the addition of NZ improved the fatigue performance and self-recovery capability of both long-term aged and moisture-damaged PA mixtures containing RAP. Future study is needed to explore the combined effect of aging and water damage on the mechanical performance of PA mixes containing high RAP contents (more than 50%).

Data Availability Statement

All data, models, and code generated or used during the study appear in the published paper.

References

AASHTO. 2014. *Standard method of test for determination of draindown characteristics in uncompacted asphalt mixtures*. AASHTO T 305. Washington, DC: AASHTO.

AASHTO. 2017a. *Standard method of test for determining the fatigue life of compacted asphalt mixtures subjected to repeated flexural bending*. AASHTO T 321-17. Washington, DC: AASHTO.

AASHTO. 2017b. *Standard method of test for determining the liquid limit of soils*. AASHTO T 89-13. Washington, DC: AASHTO.

AASHTO. 2017c. *Standard method of test for plastic fines in graded aggregates and soils by use of the sand equivalent test*. AASHTO T 176-17. Washington, DC: AASHTO.

AASHTO. 2017d. *Standard specification for stone matrix asphalt (SMA)*. AASHTO M 325-08. Washington, DC: AASHTO.

AASHTO. 2018. *Standard method of test for specific gravity and absorption of coarse aggregate (ASTM designation: C 127-12)*. AASHTO T 85-14. Washington, DC: AASHTO.

AASHTO. 2019. *Standard method of test for resistance to degradation of small-size coarse aggregate by abrasion and impact in the Los Angeles machine (ASTM C 131-01)*. AASHTO T 96-02. Washington, DC: AASHTO.

AASHTO. 2020a. *Standard method of test for determining the plastic limit and plasticity index of soils*. AASHTO T 90-20. Washington, DC: AASHTO.

AASHTO. 2020b. *Standard method of test for soundess of aggregate by use of sodium sulfate or magnesium sulfate*. AASHTO T 104-99. Washington, DC: AASHTO.

Al-Kaissi, Z. A., and O. G. Mashkoor. 2016. “Durability of porous asphalt pavement.” *J. Eng. Sustainable Dev.* 20 (4): 53–70.

Anupam, K., S. Srirangam, A. Scarpas, C. Kasbergen, and M. Kane. 2014. “Study of cornering maneuvers of a pneumatic tire on asphalt pavement surfaces using the finite element method.” *Transp. Res. Rec.* 2457 (1): 129–139. https://doi.org/10.3141/2457-14.

Arshad, A. K., J. Ahmad, and K. A. Masri. 2019. “Rutting resistance of nanosilica modified porous asphalt.” *Int. J. Civ. Eng. Technol.* 10 (1): 2274–2284.

Arshad, A. K., K. A. Masri, J. Ahmad, and M. S. Samsudin. 2017. “Dynamic modulus of nanosilica modified porous asphalt.” *IOP Conf. Ser.: Mater. Sci. Eng.* 271 (1): 012008. https://doi.org/10.1088/1757-899X/271/1/012008.

ASTM. 2011. *Standard test method for percent air voids in compacted dense and open bituminous paving mixtures*. ASTM D3203. West Conshohocken, PA: ASTM.

ASTM. 2015. *Standard test method for viscosity determination of asphalt at elevated temperatures using a rotational viscometer*. ASTM D4402M-15. West Conshohocken, PA: ASTM.

ASTM. 2017a. *Standard practice for recovery of asphalt from solution using the rotary evaporator*. ASTM D5404M-12. West Conshohocken, PA: ASTM.

ASTM. 2017b. *Standard test method for ductility of asphalt materials*. ASTM D113-17. West Conshohocken, PA: ASTM.

ASTM. 2017c. *Standard test methods for quantitative extraction of asphalt binder from asphalt mixtures*. ASTM D2172M-17. West Conshohocken, PA: ASTM.

ASTM. 2018. *Standard test method for flash and fire points by cleveland open cup tester*. ASTM D92-18. West Conshohocken, PA: ASTM.

ASTM. 2019. *Standard test method for flat particles, elongated particles, or flat and elongated particles in coarse aggregate*. ASTM D4791-19. West Conshohocken, PA: ASTM.

ASTM. 2020a. *Standard test method for effects of heat and air on asphaltic materials (thin-film oven test)*. ASTM D1754M-20. West Conshohocken, PA: ASTM.

ASTM. 2020b. *Standard test method for penetration of bituminous materials*. ASTM D5M-20. West Conshohocken, PA: ASTM.

ASTM. 2020c. *Standard test method for resistance to degradation of small-size coarse aggregate by abrasion and impact in the Los Angeles machine*. ASTM C131. West Conshohocken, PA: ASTM.

ASTM. 2020d. *Standard test method for softening point of bitumen (ring-and-ball apparatus)*. ASTM D36M-14. West Conshohocken, PA: ASTM.

ASTM. 2021. *Standard test method for specific gravity and density of semi-solid asphalt binder (pycnometer method)*. ASTM D70M-21. West Conshohocken, PA: ASTM.

Badroodi, S. K., M. R. Keymanesh, and G. Shafabakhsh. 2020. “Experimental investigation of the fatigue phenomenon in nano silica-modified warm mix asphalt containing recycled asphalt considering self-healing behavior.” *Constr. Build. Mater.* 246 (Jun): 117558. https://doi.org/10.1016/j.conbuildmat.2019.117558.

Behbahani, H., H. Ziari, N. Kamboozia, A. M. Khaki, and S. M. Mirabdolazimi. 2015. "Evaluation of performance and moisture sensitivity of glasphalt mixtures modified with nanotechnology zycosoil as an anti-stripping additive." *Constr. Build. Mater.* 78 (Mar): 60–68. https://doi.org/10.1016/j.conbuildmat.2014.12.053.

Bharath, G., K. S. Reddy, V. Tandon, and M. A. Reddy. 2021. "Aggregate gradation effect on the fatigue performance of recycled asphalt mixtures." *Road Mater. Pavement Des.* 22 (1): 165–184. https://doi.org/10.1080/14680629.2019.1620116.

Bolzan, P., J. Nicholls, and G. Huber. 2001. "Searching for superior performing porous asphalt wearing courses." In *Proc., TRB 2001 Annual Meeting*. Washington, DC: Transportation Research Board, National Research Council. CD-ROM.

Breakah, T. M., J. P. Bausano, and R. C. Williams. 2009. "Integration of moisture sensitivity testing with gyratory mix design and mechanistic-empirical pavement design." *J. Transp. Eng.* 135 (11): 852–857. https://doi.org/10.1061/(ASCE)0733-947X(2009)135:11(852).

Castro, M., and J. A. Sánchez. 2006. "Fatigue and healing of asphalt mixtures: Discriminate analysis of fatigue curves." *J. Transp. Eng.* 132 (2): 168–174. https://doi.org/10.1061/(ASCE)0733-947X(2006)132:2(168).

Daryaee, D., M. Ameri, and A. Mansourkhaki. 2020. "Utilizing of waste polymer modified bitumen in combination with rejuvenator in high reclaimed asphalt pavement mixtures." *Constr. Build. Mater.* 235 (Feb): 117516. https://doi.org/10.1016/j.conbuildmat.2019.117516.

Devulapalli, L., S. Kothandaraman, and G. Sarang. 2019. "A review on the mechanisms involved in reclaimed asphalt pavement." *Int. J. Pavement Res. Technol.* 12 (2): 185–196. https://doi.org/10.1007/s42947-019-0024-1.

Francken, L. 1979. "Fatigue performance of a bituminous road mix under realistic test conditions." *Transp. Res. Rec.* 712: 30–37.

Goh, S. W., and Z. You. 2012. "Mechanical properties of porous asphalt pavement materials with warm mix asphalt and RAP." *J. Transp. Eng.* 138 (1): 90–97. https://doi.org/10.1061/(ASCE)TE.1943-5436.0000307.

Gong, H., B. Huang, and X. Shu. 2018. "Field performance evaluation of asphalt mixtures containing high percentage of RAP using LTPP data." *Constr. Build. Mater.* 176 (Jul): 118–128. https://doi.org/10.1016/j.conbuildmat.2018.05.007.

Guo, G., and H. Zhang. 2021. "The effect of morphology of ZnO particle on properties of asphalt binder and mixture." *Int. J. Transp. Sci. Technol.* https://doi.org/10.1016/j.ijtst.2021.05.005.

Guo, M., H. Liu, Y. Jiao, L. Mo, Y. Tan, D. Wang, and M. Liang. 2020. "Effect of WMA-RAP technology on pavement performance of asphalt mixture: A state-of–the-art review." *J. Cleaner Prod.* 266 (Sep): 121704. https://doi.org/10.1016/j.jclepro.2020.121704.

Guo, M., X. Liu, Y. Jiao, Y. Tan, and D. Luo. 2021. "Rheological characterization of reversibility between aging and rejuvenation of common modified asphalt binders." *Constr. Build. Mater.* 301 (Sep): 124077. https://doi.org/10.1016/j.conbuildmat.2021.124077.

Hamedi, G. H., F. M. Nejad, and K. Oveisi. 2016. "Estimating the moisture damage of asphalt mixture modified with nano zinc oxide." *Mater. Struct.* 49 (4): 1165–1174. https://doi.org/10.1617/s11527-015-0566-x.

HasaniNasab, S., M. Arast, and M. Zahedi. 2019. "Investigating the healing capability of asphalt modified with nano-zycotherm and Forta fibers." *Case Stud. Constr. Mater.* 11 (Dec): e00235. https://doi.org/10.1016/j.cscm.2019.e00235.

Kamboozia, N., S. Mousavi Rad, and S. A. Saed. 2022. "Laboratory investigation of the effect of nano-ZnO on the fracture and rutting resistance of porous asphalt mixture under the aging condition and freeze–thaw cycle." *J. Mater. Civ. Eng.* 34 (5): 04022052. https://doi.org/10.1061/(ASCE)MT.1943-5533.0004187.

Kamboozia, N., S. A. Saed, and S. M. Rad. 2021. "Rheological behavior of asphalt binders and fatigue resistance of SMA mixtures modified with nano-silica containing RAP materials under the effect of mixture conditioning." *Constr. Build. Mater.* 303 (Oct): 124433. https://doi.org/10.1016/j.conbuildmat.2021.124433.

Kandhal, P. 2004. "Asphalt pavements mitigate tire/pavement noise." *Hot Mix Asphalt Technol.* 9 (2): 22–31.

Kandhal, P. S. 2002. *Design, construction, and maintenance of open-graded asphalt friction courses*. Greenbelt, MD: National Asphalt Pavement Association.

Kim, Y.-R., D. Little, and R. Lytton. 2003. "Fatigue and healing characterization of asphalt mixtures." *J. Mater. Civ. Eng.* 15 (1): 75–83. https://doi.org/10.1061/(ASCE)0899-1561(2003)15:1(75).

Kordi, Z., and G. Shafabakhsh. 2017. "Evaluating mechanical properties of stone mastic asphalt modified with Nano Fe_2O_3." *Constr. Build. Mater.* 134 (Mar): 530–539. https://doi.org/10.1016/j.conbuildmat.2016.12.202.

Li, R., Y. Dai, P. Wang, C. Sun, J. Zhang, and J. Pei. 2017. "Evaluation of nano-ZnO dispersed state in bitumen with digital imaging processing techniques." *J. Test. Eval.* 46 (3): 974–983. https://doi.org/10.1520/JTE20160401.

Li, R., J. Pei, and C. Sun. 2015. "Effect of nano-ZnO with modified surface on properties of bitumen." *Constr. Build. Mater.* 98 (Nov): 656–661. https://doi.org/10.1016/j.conbuildmat.2015.08.141.

Little, D. N., and A. Bhasin. 2007. "Exploring mechanism of healing in asphalt mixtures and quantifying its impact." In *Self healing materials*, 205–218. Dordrecht, Netherlands: Springer.

Ma, X., Q. Li, Y.-C. Cui, and A.-Q. Ni. 2018. "Performance of porous asphalt mixture with various additives." *Int. J. Pavement Eng.* 19 (4): 355–361. https://doi.org/10.1080/10298436.2016.1175560.

Malaysia, P. 2008. *Standard specification for road works, section 4, flexible pavement*. Kuala Lumpur, Malaysia: Jabatan. Kerja Raya Malaysia.

Mansour, T. N., and B. J. Putman. 2013. "Influence of aggregate gradation on the performance properties of porous asphalt mixtures." *J. Mater. Civ. Eng.* 25 (2): 281–288. https://doi.org/10.1061/(ASCE)MT.1943-5533.0000602.

Mansourkhaki, A., M. Ameri, and D. Daryaee. 2019. "Application of different modifiers for improvement of chemical characterization and physical-rheological parameters of reclaimed asphalt binder." *Constr. Build. Mater.* 203 (Apr): 83–94. https://doi.org/10.1016/j.conbuildmat.2019.01.086.

Masri, K. A., A. K. Arshad, and M. S. Samsudin. 2016. "Mechanical properties of porous asphalt with nanosilica modified binder." *Jurnal Teknologi* 78 (7–2): 139–146. https://doi.org/10.11113/jt.v78.9509.

Masri, K. A., S. M. Z. N. Syafiqah, M. A. Seman, P. J. Ramadhansyah, H. Yaacob, and N. Mashros. 2021. "A review on nanomaterials as additive in asphalt binder." *IOP Conf. Ser.: Earth Environ. Sci.* 682 (1): 012055. https://doi.org/10.1088/1755-1315/682/1/012055.

Moniri, A., H. Ziari, M. R. M. Aliha, and Y. Saghafi. 2021. "Laboratory study of the effect of oil-based recycling agents on high RAP asphalt mixtures." *Int. J. Pavement Eng.* 22 (11): 1423–1434. https://doi.org/10.1080/10298436.2019.1696461.

Mullapudi, R. S., P. S. Chowdhury, and K. S. Reddy. 2020. "Fatigue and healing characteristics of RAP binder blends." *J. Mater. Civ. Eng.* 32 (8): 04020214. https://doi.org/10.1061/(ASCE)MT.1943-5533.0003284.

Paluri, Y., V. Noolu, H. Mudavath, and R. Kumar Pancharathi. 2021. "Flexural fatigue behavior of steel fiber-reinforced reclaimed asphalt pavement–based concrete: An experimental study." *Pract. Period. Struct. Des. Constr.* 26 (1): 04020053. https://doi.org/10.1061/(ASCE)SC.1943-5576.0000540.

Poulikakos, L. D., and M. N. Partl. 2009. "Evaluation of moisture susceptibility of porous asphalt concrete using water submersion fatigue tests." *Constr. Build. Mater.* 23 (12): 3475–3484. https://doi.org/10.1016/j.conbuildmat.2009.08.016.

Sadeghnejad, M., and G. Shafabakhsh. 2017. "Use of Nano SiO_2 and Nano TiO_2 to improve the mechanical behaviour of stone mastic asphalt mixtures." *Constr. Build. Mater.* 157 (Dec): 965–974. https://doi.org/10.1016/j.conbuildmat.2017.09.163.

Saed, S. A., N. Kamboozia, and S. Mousavi Rad. 2022a. "Performance evaluation of stone matrix asphalt mixtures and low-temperature properties of asphalt binders containing reclaimed asphalt pavement materials modified with nanosilica." *J. Mater. Civ. Eng.* 34 (1): 04021380. https://doi.org/10.1061/(ASCE)MT.1943-5533.0004016.

Saed, S. A., H. R. Karimi, S. M. Rad, M. R. A. Aliha, X. Shi, and P. J. Haghighatpour. 2022b. "Full range I/II fracture behavior of asphalt mixtures containing RAP and rejuvenating agent using two different

3-point bend type configurations." *Constr. Build. Mater.* 314 (Jan): 125590. https://doi.org/10.1016/j.conbuildmat.2021.125590.

Shadman, M., and H. Ziari. 2017. "Laboratory evaluation of fatigue life characteristics of polymer modified porous asphalt: A dissipated energy approach." *Constr. Build. Mater.* 138 (May): 434–440. https://doi.org/10.1016/j.conbuildmat.2017.02.043.

Shafabakhsh, G. A., M. Sadeghnejad, B. Ahoor, and E. Taheri. 2020. "Laboratory experiment on the effect of nano SiO_2 and TiO_2 on short and long-term aging behavior of bitumen." *Constr. Build. Mater.* 237 (Mar): 117640. https://doi.org/10.1016/j.conbuildmat.2019.117640.

Shafabakhsh, G. H., O. J. Ani, and M. Talebsafa. 2015. "Artificial neural network modeling (ANN) for predicting rutting performance of nano-modified hot-mix asphalt mixtures containing steel slag aggregates." *Constr. Build. Mater.* 85 (Jun): 136–143. https://doi.org/10.1016/j.conbuildmat.2015.03.060.

Shen, S., and T. Sutharsan. 2011. "Quantification of cohesive healing of asphalt binder and its impact factors based on dissipated energy analysis." *Road Mater. Pavement Des.* 12 (3): 525–546. https://doi.org/10.1080/14680629.2011.9695259.

Slebi-Acevedo, C. J., P. Lastra-González, I. Indacoechea-Vega, and D. Castro-Fresno. 2020. "Laboratory assessment of porous asphalt mixtures reinforced with synthetic fibers." *Constr. Build. Mater.* 234 (Feb): 117224. https://doi.org/10.1016/j.conbuildmat.2019.117224.

Sun, Y., W. Wang, and J. Chen. 2019. "Investigating impacts of warm-mix asphalt technologies and high reclaimed asphalt pavement binder content on rutting and fatigue performance of asphalt binder through MSCR and LAS tests." *J. Cleaner Prod.* 219 (May): 879–893. https://doi.org/10.1016/j.jclepro.2019.02.131.

Van Dijk, W., H. Moreaud, A. Quedeville, and P. Uge. 1972. "The fatigue of bitumen and bituminous mixes." In *Proc., 3rd Int. Conf. on the Structural Design of Asphalt Pavements*. Washington, DC: National Academies of Science, Engineering, and Medicine.

Voskuilen, J. L. M., and P. N. W. Verhoef. 2003. "Causes of premature ravelling failure in porous asphalt." In *Proc., 6th Int. RILEM Symp. on Performance Testing and Evaluation of Bituminous Materials*, 191–197. Zurich, Switzerland: International Union of Laboratories and Experts in Construction Materials, Systems and Structures.

Wan, P., Q. Liu, S. Wu, Z. Zhao, S. Chen, Y. Zou, W. Rao, and X. Yu. 2021. "A novel microwave induced oil release pattern of calcium alginate/nano-Fe_3O_4 composite capsules for asphalt self-healing." *J. Cleaner Prod.* 297 (May): 126721. https://doi.org/10.1016/j.jclepro.2021.126721.

Wu, J., Y. Wang, Q. Liu, Y. Wang, C. Ago, and M. Oeser. 2020. "Investigation on mechanical performance of porous asphalt mixtures treated with laboratory aging and moisture actions." *Constr. Build. Mater.* 238 (Mar): 117694. https://doi.org/10.1016/j.conbuildmat.2019.117694.

Xu, H., W. Guo, and Y. Tan. 2015. "Internal structure evolution of asphalt mixtures during freeze–thaw cycles." *Mater. Des.* 86 (Dec): 436–446. https://doi.org/10.1016/j.matdes.2015.07.073.

Xu, H., W. Guo, and Y. Tan. 2016. "Permeability of asphalt mixtures exposed to freeze–thaw cycles." *Cold Reg. Sci. Technol.* 123 (Mar): 99–106. https://doi.org/10.1016/j.coldregions.2015.12.001.

Xu, S., X. Liu, A. Tabaković, and E. Schlangen. 2020. "A novel self-healing system: Towards a sustainable porous asphalt." *J. Cleaner Prod.* 259 (Jun): 120815. https://doi.org/10.1016/j.jclepro.2020.120815.

Xu, S., X. Liu, A. Tabaković, and E. Schlangen. 2021. "Experimental investigation of the performance of a hybrid self-healing system in porous asphalt under fatigue loadings." *Materials* 14 (12): 3415. https://doi.org/10.3390/ma14123415.

Yousefi, A., A. Behnood, A. Nowruzi, and H. Haghshenas. 2021. "Performance evaluation of asphalt mixtures containing warm mix asphalt (WMA) additives and reclaimed asphalt pavement (RAP)." *Constr. Build. Mater.* 268 (Jan): 121200. https://doi.org/10.1016/j.conbuildmat.2020.121200.

Zhang, H., K. Anupam, A. Scarpas, C. Kasbergen, and S. Erkens. 2020. "Effect of stone-on-stone contact on porous asphalt mixes: Micromechanical analysis." *Int. J. Pavement Eng.* 21 (8): 990–1001. https://doi.org/10.1080/10298436.2019.1654105.

Zhang, H., Y. Gao, G. Guo, B. Zhao, and J. Yu. 2018. "Effects of ZnO particle size on properties of asphalt and asphalt mixture." *Constr. Build. Mater.* 159 (Jan): 578–586. https://doi.org/10.1016/j.conbuildmat.2017.11.016.

Zhang, H., C. Zhu, J. Yu, B. Tan, and C. Shi. 2015. "Effect of nano-zinc oxide on ultraviolet aging properties of bitumen with 60/80 penetration grade." *Mater. Struct.* 48 (10): 3249–3257. https://doi.org/10.1617/s11527-014-0395-3.

Zhang, K., Y. Liu, S. Nassiri, H. Li, and K. Englund. 2021. "Performance evaluation of porous asphalt mixture enhanced with high dosages of cured carbon fiber composite materials." *Constr. Build. Mater.* 274 (Mar): 122066. https://doi.org/10.1016/j.conbuildmat.2020.122066.

Ziari, H., M. Aliha, A. Moniri, and Y. Saghafi. 2020a. "Crack resistance of hot mix asphalt containing different percentages of reclaimed asphalt pavement and glass fiber." *Constr. Build. Mater.* 230 (Jan): 117015. https://doi.org/10.1016/j.conbuildmat.2019.117015.

Ziari, H., A. Amini, and A. Goli. 2020b. "The effect of different aging conditions and strain levels on relationship between fatigue life of asphalt binders and mixtures." *Constr. Build. Mater.* 244 (May): 118345. https://doi.org/10.1016/j.conbuildmat.2020.118345.

Ziari, H., A. Moniri, P. Bahri, and Y. Saghafi. 2019. "The effect of rejuvenators on the aging resistance of recycled asphalt mixtures." *Constr. Build. Mater.* 224 (Nov): 89–98. https://doi.org/10.1016/j.conbuildmat.2019.06.181.